Robotic System for Automated Visual Detection of Physical Instability in Protein Systems

Stefan Ilic[a], Johann Buczkowski[b], Jiahong Wang[c], Francesco Nonis[a], Cécile Gehin-Delval[d], Giulia Marchesini[b], Josie Hughes[a]

[a]*EPFL, Rte Cantonale, Lausanne, 1015, Vaud, Switzerland*
[b]*Nestlé Research, Rte de Jorat 52, Lausanne, 1000, Vaud, Switzerland*
[c]*Max Planck Institute for Informatics, Saarbrücken, 66123, Germany*
[d]*Société des Produits Nestlé S.A., Nestlé Product Technology Centre Coffee, Rte de Chavornay 3, Orbe, 1350, Vaud, Switzerland*

Abstract

Evaluating the physical instability of protein dispersions is critical in food science and product development, yet current methods rely on subjective visual inspection or costly light-scattering instruments. These approaches provide only snapshots in time and offer limited temporal resolution. We present a robotic and computer vision system for automated assessment of the physical instability of protein dispersions across varying pH conditions. The system automates titration and pipetting tasks, while an optical camera continuously monitors up to ten samples stored in cuvettes. Captured images are analyzed with a Laplacian-based algorithm that enhances agglomerate visibility and quantifies instability through a single metric. The system was validated through acid titration of a 1% milk protein solution at 30°C, successfully detecting both massive physico-chemical instability (aggregation) and subtle physical instability (sedimentation). The amount of added acid required to reach the instability point showed a 6% variation in the millimolar range, demonstrating high reproducibility across experiments. This cost-effective and scalable platform enables parallel analysis of up to ten samples, making it well suited for early-stage formulation screening. Beyond protein dispersions, the system could be extended to study more complex, multi-ingredient formulations. In addition, it can facilitate the generation of large, high-quality datasets to support the development of machine-learning models for formulation optimization.

1. Introduction

Preventing physical instability in food systems such as emulsions, dairy drinks, sauces and dressings, is essential for maintaining their structure and functionality (Dickinson, 2015), (Zhu et al., 2022). Instabilities like creaming, sedimentation or phase separation can compromise product quality through its life-cycle. During production, preserving product stability ensures uniform mixing and consistent batch quality, while over shelf-life, it affects key sensory attributes like appearance, texture and mouthfeel, critical drivers of consumer preference (McNally et al., 2007). As a result, physical instability is a critical attribute in product development influenced by several factors, including temperature, concentration and processing conditions (Everett, 2007). This instability is typically assessed through human visual inspection, an imprecise but simple and effective method for early-stage evaluation (Mcclements, 2007), (Den Engelsman et al., 2011). This is often complemented by advanced physico-chemical characterization techniques, mainly

based on light scattering technologies such as Dynamic Light Scattering (DLS) and Laser Granulometry, as well as other methods like spectrophotometry (Matusiak & Grzadka, 2017), (Housmans et al., 2023), (Alexander & Dalgleish, 2006). In the pharmaceutical industry, high-throughput well plate systems based on these technologies are routinely used for screening therapeutic proteins (Dauer, Kamm, et al., 2021), peptides (Chaudhuri et al., 2014), and monoclonal antibodies (Dauer, Pfeiffer-Marek, et al., 2021). While these advanced technologies provide objective and robust assessments, they involve high operational costs related to equipment and skilled labor, limiting their use in food science to specific high-added value cases. As a result, much of the stability assessment still relies on visual inspection, an approach limited by subjectivity and high risk of error, especially in complex or continuous systems where the transition between stable and unstable states is gradual and not visually apparent. This risk is heightened during prolonged monitoring or when handling large number of samples, as sustained observation under challenging lighting conditions can cause operator fatigue, compromising accuracy and reliability (Grandjean, 1979). Furthermore, both visual and analytical approaches provide only discrete snapshots, lacking the real-time capability to capture how stability evolves over time. These limitations, combined with relatively low-throughput, force scientists and product developers to compromise and restrict their design space. This has initiated the exploration of alternative methods to provide objective, metric-based insights into physical stability of liquid systems.

The use of computer vision in food science and industrial food production has primarily focused on enhancing food quality assessment (Sun, 2016). This technology provides a low-cost, non-destructive method for estimating product quality by leveraging conventional cameras, as well as spectroscopic and hyperspectral imaging technologies (Hassoun et al., 2023). When integrated with image analysis algorithms, these systems enable image segmentation and object classification including estimation of weight and color (He et al., 2013), (D. Wu & Sun, 2013). As a result, these methods can be applied across a diverse range of food products, including fruits, vegetables, meat and dairy (Bhargava & Bansal, 2021), (Shi et al., 2021), (Milovanovic et al., 2021). Beyond quality control, computer vision is also employed in food handling and packaging, where visual recognition systems enable precise pick-and-place operations on production lines (Wang et al., 2022). In the domain of food science, the use of computer vision remains rather scarce. A system that combines robotics, computer vision and machine learning has been developed for the specific assessment of beer quality based on foamability (Gonzalez Viejo et al., 2018). A robotic pourer ensures repeatability across experiments, while an array of sensors, combined with a camera, computer vision algorithm, and Near Infrared Spectroscopy, captures both the physical and chemical foam properties. Despite these advancements, the adoption of robots in food laboratories remains limited, failing to replicate successes in analytical chemistry (Abolhasani & Kumacheva, 2023), material science (Burger et al., 2020) and pharmaceuticals (Alexovič et al., 2018), (Alexovič et al., 2020). Much of the experimentation remains manual and time-consuming, leading to compromised repeatability and reduced throughput. However, the integration of robotics for experiment automation and computer vision for visual assessment could significantly streamline workflows, enhancing both efficiency and accuracy (Holland & Davies, 2020).

Driven by growing consumer demand and sustainability goals, the food industry has increasingly focused on developing products based on alternative proteins (Schmitt et al., 2021). A major focus in this area is the characterization and formulation of new protein ingredients, where solubility is one of the most critical techno-functional properties in

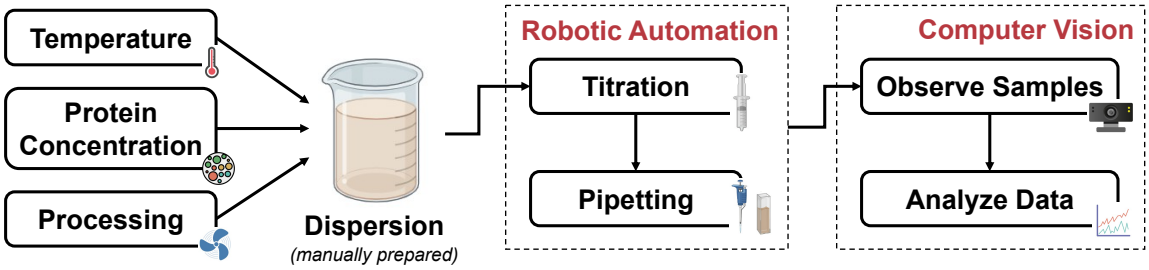

Figure 1: The process for detecting physical instability in protein systems.

food science and formulation (Wijaya et al., 2017), (Yan et al., 2020). To help address this challenge and accelerate the development of optimal protein-based liquid formulations, we developed an automated system that combines robotics and computer vision for visual assessment of physical instability across varying pH conditions, as shown on Figure 1. The robotic component enables precise and efficient titration and pipetting, while computer vision provides real-time, quantitative and simultaneous monitoring of physical instability across multiple samples. Using an edge detection image analysis algorithm, the system quantifies stability through a single metric, tracking its progression over time and identifying formation of aggregates. High accuracy and reproducibility were observed across experiments, with the instability point detected at the identical pH and a $\pm 6\%$ variation in titrant volume. This highlights the potential of robotics and computer vision to provide a cost-efficient alternative to traditional light-scattering techniques, with the main cost differentiator lying in the use of standard Complementary Metal-Oxide-Semiconductor (CMOS) imaging rather than specialized optical instrumentation.

In the remainder of the paper, we first introduce the robotic system and describe the computer vision methodology, along with the physical instability detection algorithm. We then evaluate the system's performance by first assessing the consistency of stability measurements across stable samples prepared in multiple batches. This is followed by an evaluation of its effectiveness in detecting physical instability and the repeatability of experimental results. Finally, we conclude with a discussion of potential improvements to the robotic setup and future applications of the computer vision technology.

2. Materials and Methods

2.1. Physical Instability: Background

Physical instability occurs when dispersions lose uniformity due to sedimentation or aggregation (Ryan & Foegeding, 2015). Preventing this phenomenon is essential in beverage formulation to preserve product appearance and long shelf life (Molet-Rodríguez et al., 2018). Stability is influenced by several factors, including temperature, protein concentration and processing conditions, which progressively accelerate aggregation (Cosgrove, 2010). A transition zone between stable and unstable states is of interest in food science, as it offers opportunities to optimize formulations for both cost and nutritional value.

2.2. Robotic Automation

The assessment of physical instability typically involves a pH-titration experiment, where an acid or alkali is added to a temperature-controlled vessel containing the test sample to adjust the pH. The sample is titrated to a specific pH level, then pipetted into a cuvette, a high optical clarity container, where it is examined either visually by a human or using specialized laboratory equipment. If the sample appears stable, titration continues until instability is observed.

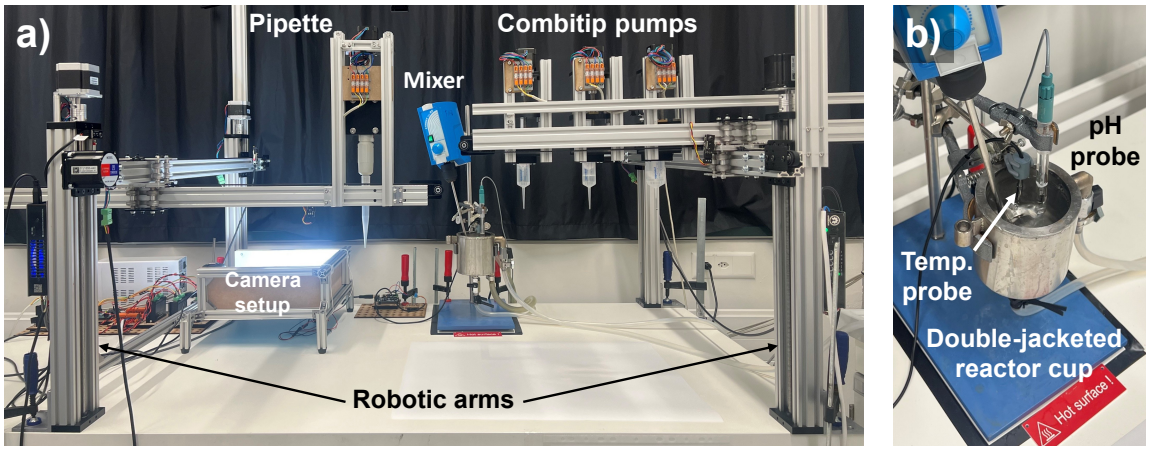

Figure 2: The robotic system for automated titration, monitoring, and detection of physical instability.

The automation of this process required bimanual manipulation to control both the addition of titrant into the heated vessel and the pipetting of the sample into the cuvettes. To ensure precise control and achieve lower system cost, we developed a dual 3 Degree of Freedom (DoF) robotic arm system based upon Cartesian robot principles (Müller et al., 2023), as seen on Figure 2 a). The right arm was equipped with three custom Combitip pumps for titrant dispensing, while the left arm held an automated pipette. Both arms operated within a shared workspace that housed a temperature-controlled double-jacketed reactor cup, where the analyzed sample was actively stirred. To ensure accuracy and prevent sample fluctuations, both pH and temperature were continuously recorded. Instability monitoring was performed using a camera setup, where cuvettes were observed by an CMOS camera under controlled lighting conditions and analyzed with a computer vision algorithm. The robotic system was exclusively validated for acid titrations, with no inherent limitations preventing its use for other types of titrations.

2.2.1. pH and Temperature Monitoring

Temperature was captured using a DS18B20 probe (Velleman, Beveren, Belgium), while pH measurements were taken with a porotrode pH sensor Metrohm AG, Herisau, Switzerland connected to a pH amplifier (DFRobot, Shanghai, China). The pH and temperature probes, immersed in the sample, provided readings every second to ensure continuous monitoring and early detection of unexpected anomalies. The system operated under stable temperature conditions that can be adjusted depending on the formulation and experimental objective. However, pH changed significantly during the experiment as the sample was titrated to a target pH value. The experiment proceeded only once the target pH was reached and readings were stable, with stability defined as no variation beyond a 0.03 threshold in the last 30 measurements. The pH probe was calibrated daily using pH 4 and pH 7 buffers (Merck, KGaA, Darmstadt, Germany).

2.2.2. pH Adjustment

A proportional controller was employed to achieve the target pH, assuming a linear relationship between pH and the volume of added titrant. The proportional controller parameter, k_p, was independently calculated for each experiment. Additionally, it was adjusted at each titration step, with $k_{p(n+1)}$ for the next acid titration step determined using the following equation:

$$k_{p(n+1)} = \frac{\sum_{i=1}^{n} V_{acid(i)}}{pH_{start} - pH_{current}} \tag{1}$$

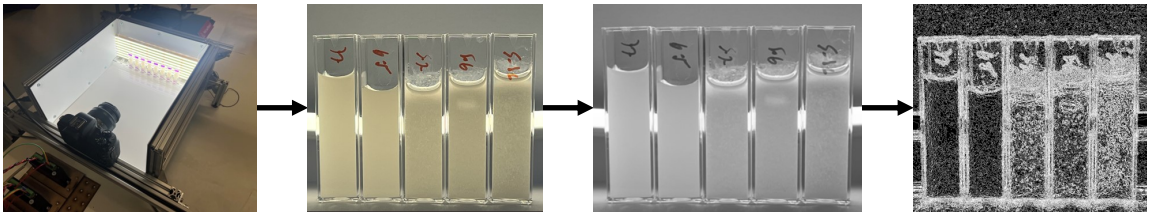

Figure 3: Computer vision pipeline for detection of physical instability using a Laplacian filter.

where $\sum V_{acid(i)}$ is the total volume of added acid up to the last titrated step n, while pH_{start} and $pH_{current}$ denote the pH measured at the start of the experiment and at the current titration step, respectively. For the first titrated cuvette, $\sum V_{acid(i)}$ was equal to $V_{acid\ start}$, a user-defined initial volume of acid, dispensed to enable accurate calculation of the control parameter while avoiding pH overshoot.

Upon identifying the control parameter $k_{p(n+1)}$ for the subsequent titration step, the volume of acid to be dispensed $V_{adjust(n+1)}$ was calculated using the following equation:

$$V_{acid(n+1)} = k_{p(n+1)} \cdot (pH_{current} - pH_{target(n+1)}) \tag{2}$$

where $pH_{target(n+1)}$ is the pH to be reached in the subsequent n+1 titration step.

This process was repeated across titration steps until all user-defined pH targets were reached. The same pH adjustment approach can also be adapted for alkali titrations with minor modifications, as the pH increases rather than decreases.

2.3. Computer Vision and Detection of Physical Instability

Visual detection of physical instability relies on detecting particles and their distribution throughout the liquid, (Tadros, 2007). To detect these behaviors, we developed a computer vision pipeline that identifies particle aggregation under controlled lighting conditions. This approach focuses solely on the visual detection of aggregates rather than direct measurement of particle size, using a Laplacian filter to enhance contrast and highlight aggregates. Commonly employed in computer vision for edge detection and image sharpening, this filter emphasizes abrupt intensity changes that correspond to edges or fine details (Bovik, 2010), (Shrivakshan & Chandrasekar, 2012). By applying this technique, subtle features such as early stage aggregates or phase separation were detected, revealing fine details that would otherwise remain undetectable in the raw image. In practical terms, stable dispersions yield consistent Laplacian readings, whereas the onset of instability causes noticeable fluctuations as aggregates form. However, due to its sensitivity to noise, the Laplacian filter is often combined with Gaussian filtering to smooth the image and reduce noise, improving the overall detection accuracy (Bovik, 2010). The Laplacian was selected as a training-free, low-parameter method that emphasizes intensity gradients associated with visible aggregates. Alternative approaches such as Canny, Fourier-based, or Convolutional Neural Networks (CNN's) typically require additional threshold tuning, frequency calibration, or large labeled datasets, which extend beyond the scope of the present work, (Szeliski, 2022).

The process began with capturing images of cuvettes positioned in a controlled lightning environment, where a strong backlight enhanced the visibility of agglomerates. Following this, a computer vision pipeline, shown in Figure 3, was applied. First, the captured images were denoised using a Gaussian filter which removed intensity variations. These images were then converted to grayscale, reducing them to a single channel, decreasing computational load while emphasizing intensity variations and detection of

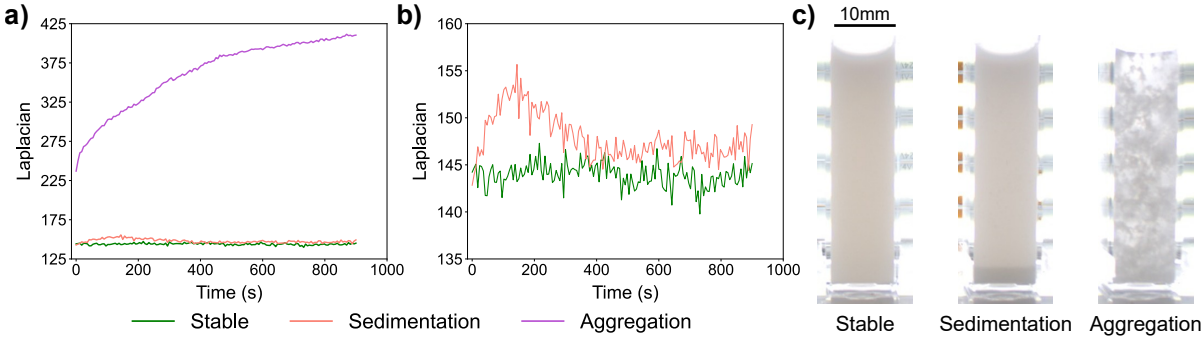

Figure 4: (a, b) Raw Laplacian readings for stable, sedimented and aggregated samples. (c) Images of samples stored in a cuvette, including a stable, a sedimented, and an aggregated sample.

subtle changes. Finally, a Laplacian filter was applied to highlight regions of rapid intensity change. As a second-order derivative filter, it enhanced the edges of features within the image, emphasizing changes in the liquid, such as the presence of agglomerates. The resulting image was thresholded to enhance edge visibility, making it easier for human interpretation. However, the pixel values, which represent the edge intensity, also enabled the quantification of the sample's stability through a single numerical metric. Given an image J, the Laplacian result $L(x, y)$ for a pixel (x, y) was calculated as:

$$L(x, y) = \frac{\partial^2 J(x, y)}{\partial x^2} + \frac{\partial^2 J(x, y)}{\partial y^2} \tag{3}$$

The quantitative metric representing stability M_J for image J was calculated as the average of absolute values of the Laplacian response $L_J(x_i, y_i)$ at pixel i in image J as seen below:

$$M_J = \frac{1}{N} \sum_{i=1}^{N} |L_J(x_i, y_i)| \tag{4}$$

where N is the total number of pixels on the image or within specified region of interest.

2.3.1. Laplacian and Sample Stability

Using the proposed computer vision algorithm, a stable sample (1% milk protein dispersion at pH 7.2.) was characterized by consistent Laplacian readings, as illustrated in Figure 4 a) and b). In contrast, an extreme form of instability, known as physico-chemical instability or aggregation, was indicated by a continuous and rapid rise in Laplacian readings. This type of instability was visually distinct, as the sample appears heterogeneous, with the ongoing motion of agglomerates in the liquid contributing to a continuous rise in Laplacian readings. When physical instability occurred in a subtle form, such as sedimentation (Figure 4 c), it initially caused a rapid increase in Laplacian readings before stabilizing at nominal values. This pattern occurred since particles were initially dispersed throughout the liquid but gradually settle at the bottom of the cuvette, after which both sedimentation and changes in Laplacian readings became minimal.

2.3.2. Temporal Instability

Comparing raw Laplacian readings can be challenging, as they are sensitive to differences in batches, formulation or cuvette positioning in the camera setup. Although formulation and batch effects require separate experiments, normalizing Laplacian readings within each cuvette reduces variability caused by positional differences. For this purpose, we introduced the Temporal Instability metric (I_T), which compares each Laplacian reading for a given cuvette to its initial measurement within the same experiment. By

aligning all samples to a common baseline, this metric enables comparison across cuvettes and experiments, with substantial changes in I_T corresponding to sedimentation or other instability events. The metric, calculated for a single cuvette, was defined as follows:

$$I_T = \left| \frac{M_i - M_1}{M_1} \right| \tag{5}$$

where M_i is the Laplacian for the current image i, while M_1 is the first Laplacian reading.

To assess instability, a sample was monitored over a time period t, with a total of U images captured at a user-defined time interval τ.

$$U = \frac{t}{\tau} \tag{6}$$

A sample was considered unstable when at least P of the last k images had Temporal Instability metric exceeding the limit θ:

$$\sum_{i=U-k}^{U} 1(I_T > \theta) \geq P, \begin{cases} 1, & I_T > \theta \\ 0, & I_T \leq \theta \end{cases} \tag{7}$$

This limit was derived from a separate calibration test conducted prior to the main experiment using V (ten) stable samples of the same formulation under identical conditions (temperature and batch). Each sample was placed in a cuvette in the camera setup and monitored up to 60 minutes. The boundaries were first determined at the sample (cuvette) level across all images and then compared across V samples, minimizing false positives. The resulting limit θ was defined as follows:

$$\begin{aligned} &\theta > T_T \times N_T \\ &N_T = \max_{c=1,\ldots,V} \left(\frac{\sigma(M_c)}{\overline{M_c}} \right), \end{aligned} \tag{8}$$

where $\sigma(M_c)$ is the standard deviation and $\overline{M_c}$ is the mean of all Laplacian readings at the sample level. The highest measured temporal noise N_T was used to calculate the limit, with the confidence threshold T_T typically set to 3, corresponding to 3σ. This threshold ensured that the Temporal Instability readings of stable samples of formulations within the same product group remain within the limit θ. Ideally, this calibration should be performed for each formulation. When visual properties such as color and turbidity are comparable, the limit derived from one formulation can also be applied to others within the same product group.

2.4. Hardware Implementation

2.4.1. Cartesian Robotic Arms

The experimental process was automated using two custom 3-Degrees-of-Freedom (DoF) Cartesian robotic arms providing linear XYZ motion, as shown in Figure 2. Unlike traditional 6-DoF robotic arms, these Cartesian robots allow mounting of multiple devices. If the capacity of a single arm is exceeded, additional arms can be added to accommodate the equipment and collaborate within overlapping workspaces. Controlling dual 3-DoF Cartesian robots is significantly easier than operating two 6-DoF robotic arms, as their linear motion and simple physical structure require no complex motion planning. The control system operates through user-defined waypoints, with the arms executing programmed movements between specified positions.

Combitip Volume	Minimum Dispensing Volume	Precision (Standard Deviation σ)	Accuracy
25 mL	0.5 mL	0.04 mL	$\pm$ 0.1 mL
50 mL	1 mL	0.05 mL	$\pm$ 0.1 mL

Table 1: Technical specifications of 25 and 50 mL custom Combitip pumps.

2.4.2. Laboratory Equipment

The robotic setup included laboratory equipment for pH and temperature monitoring, along with a custom stainless steel jacketed reactor cup connected to a circulating bath (Haake Technik GmbH, Vreden, Germany), maintaining sample temperature within $\pm 0.3°C$. Unlike conventional glass reactor cups, this design featured additional inlet and outlet ports, allowing easy cleaning when connected to a water source. All laboratory equipment was mounted on a stand within the overlapping workspace of the two Cartesian robotic arms, except for the circulating bath, which was placed below the table.

2.4.3. Dispensing and Pipetting Automation

The robotic system used one 50 mL and two 25 mL custom Combitip pumps for precise, automated titrant dispensing, with pump characteristics detailed in Table 1. Combitips (Eppendorf AG, Hamburg, Germany) were selected over syringes for their superior precision and accuracy, providing an immediate response to linear motion. Precision and absolute error were determined by repeatedly dispensing the minimum volume and measuring the dispensed mass. The use of multiple Combitip pumps ensured sufficient titrant volume across a range of formulations to reach instability, while also providing flexibility in reagent type and concentration. In addition to titrant dispensing, sample collection was automated using Calibra 832 1-10 mL pipette (Socorex, Ecublens, Switzerland). Both the pipette and Combitip pumps operated via a stepper motor and linear screw mechanism, converting rotational motion into linear displacement to press the pipette button or move the Combitip plunger.

2.4.4. Camera Setup

Sample monitoring and physical instability detection were performed using a custom camera setup. A total of 10 samples, each stored in a 4 mL polystyrene cuvette (Sarstedt, Nümbrecht, Germany), were observed using an industrial CMOS camera equipped with an 8mm fixed focal length lens (both from Basler AG, Ahrensburg, Germany) to minimize

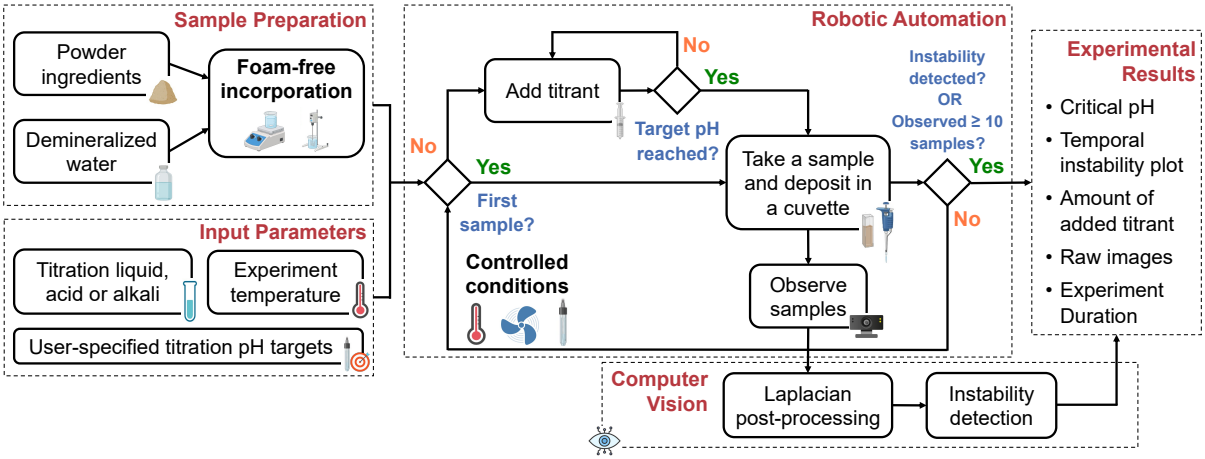

Figure 5: Automated experimental process for detecting physical instability in protein systems using computer vision, starting from a manually prepared sample.

image distortion. The camera captured 4K images every 6 seconds, which were then transferred to a computer for further analysis. Given that optimal lighting conditions were crucial for detecting visual changes in the samples, a set of LED strips was positioned behind the cuvettes to provide controlled illumination. A transparent acrylic holder kept the cuvettes in place, maintaining consistent positioning required for robotic automation.

2.5. Analyzed Proteins and Titration Liquids

To evaluate the performance of the robotic system, a stability analysis was conducted on milk protein concentrate (MPC), 4861, 81.4% protein (Fonterra, Auckland, New Zealand). Titration process was performed using 0.1 mol/L Hydrocholoric Acid (HCl) (Merck, KGaA, Darmstadt, Germany).

2.6. Experimental Process

The experimental process, shown in Figure 5, began by manually dissolving MPC in deionized water on a magnetic stirrer for one hour at ambient temperature. After confirming complete dissolution (no visible lumps in the dispersion), a 400 g sample was transferred into a double-jacketed reactor cup at 30°C and stirred at 150-200 RPM using an overhead stirrer. The sample was heated to a target temperature defined before the experiment according to the formulation and experimental objective. Once temperature of the dispersion was stable, the automated titration process began. The first cuvette contained the native sample, while the remaining cuvettes were reserved for samples titrated to user-defined pH values, set prior to the experiment. After titration to a target pH, the corresponding sample was pipetted into a cuvette within the camera setup, where it was monitored for 15 minutes. Images were captured every 6 seconds, and a sample was considered unstable if at least five last images show Temporal Instability above the threshold. The titration stopped if instability was detected in two consecutive cuvettes, with evaluation continuing until the last stable cuvette was observed for 15 minutes, as instability may develop over time.

To identify the instability point and determine the transition zone between stable and unstable states, the titration experiment was performed in two stages. The first experiment broadly investigated the pH range using 0.5 pH unit steps to locate the instability region, while the second experiment used 0.1 pH unit steps to precisely detect the instability point. Between experiments, the pH 7 buffer solution was used to confirm the pH probe was free of protein aggregates and unaffected by signal drift.

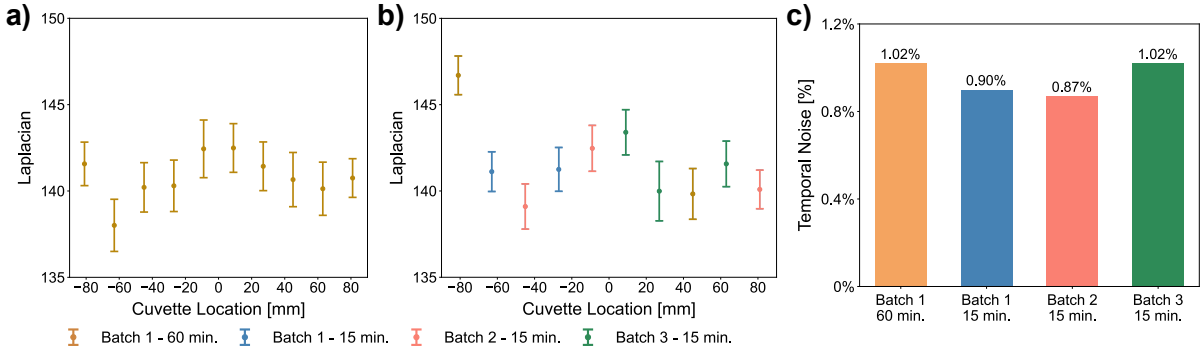

Figure 6: (a) Temporal and spatial noise recorded while observing an identical sample over 60 minutes and (b) three independently prepared samples over 15 minutes. (c) The maximum standard deviation of Laplacian readings at the cuvette level across all observed samples, referred to as Temporal Noise.

3. Results

3.1. Stability of Laplacian Readings

The absolute Laplacian measurements are influenced by the varying distance of cuvettes relative to the camera. To investigate these spatial effects, we monitor samples from three separately prepared MPC batches over 15 and 60 minutes. When analyzing samples from the identical batch for 60 minutes (Figure 6 a), mean Laplacian readings vary by 3% between samples. Similarly, when evaluating samples from three different batches over 15 minutes (Figure 6 b), mean Laplacian readings show a 5.2% variation, with samples randomly distributed across cuvettes. However, the standard deviation of Laplacian readings at the cuvette level, referred to as temporal noise N_T, remains stable, with only absolute Laplacian readings varying between cuvettes. As illustrated in Figure 6 c), temporal noise remains consistently close to 1%, regardless of observation time, cuvette position or batch differences. Using the data treatment described in Equation 8, we establish the instability detection threshold θ to be 3.5% for $\pm 3\sigma$ confidence.

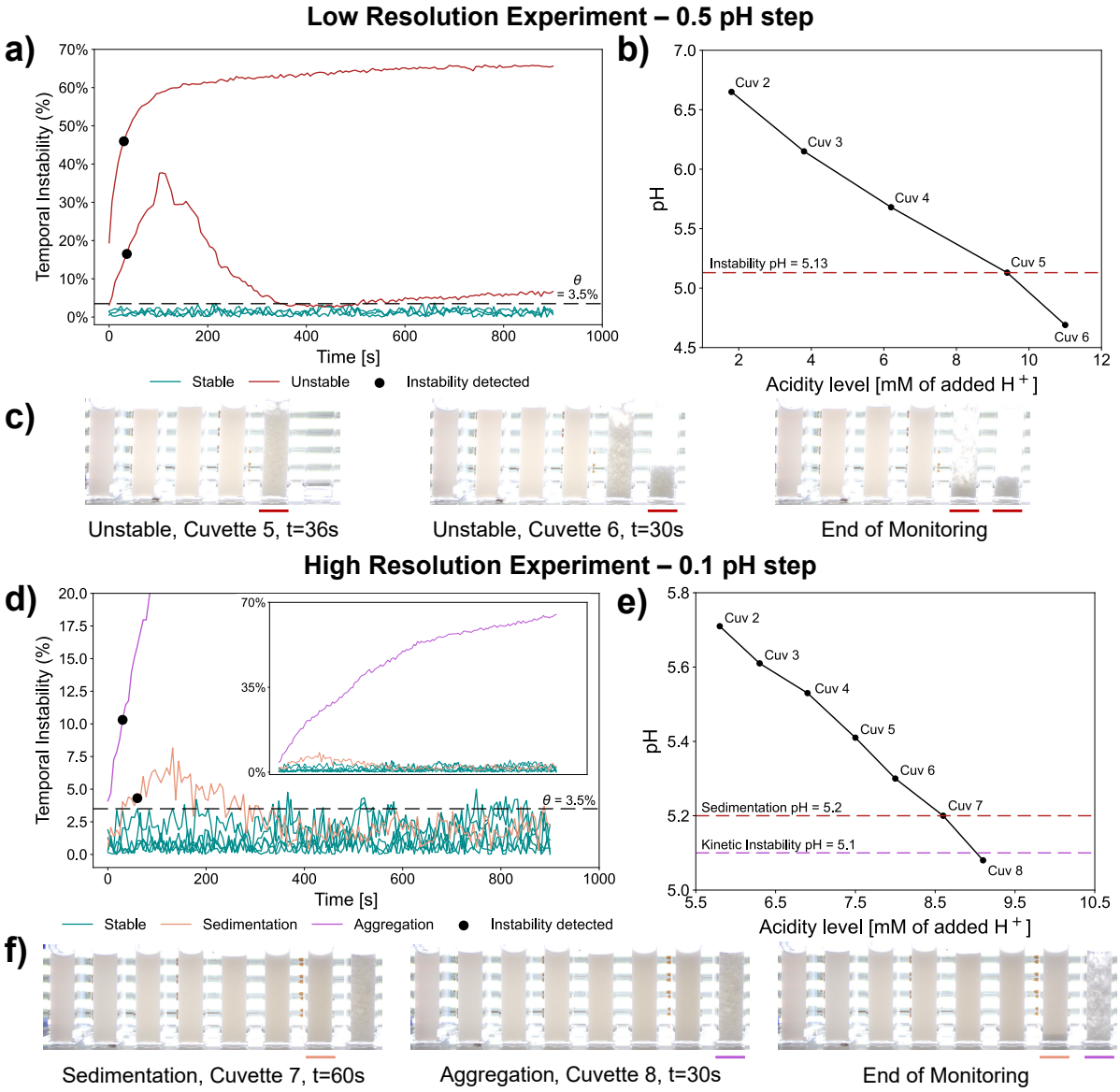

Figure 7: Titration data of low and high resolution titration experiments for milk protein dispersion. (a)(d) Temporal instability evolution, (b)(e) titration curve and (c)(f) raw images of samples.

3.2. Automated Instability Detection

To assess the robotic system's ability to detect physical instability, MPC was titrated at 30°C, with each sample monitored for 15 minutes. An initial titration experiment using a 0.5 pH step was conducted to roughly identify the instability region, followed by a high-resolution 0.1 pH step experiment to precisely determine the critical pH, defined as the pH at which the dispersion instability becomes visible.

In the initial low pH resolution experiment, the instability was detected between pH 5.68 (cuvette 4, last stable sample) and pH 5.13 (cuvette 5, first unstable sample), as shown in Figure 7 a), b) and c). The detected instability corresponded to the massive protein aggregation, resulting in phase separation with most of the aggregated protein settling at the bottom of the cuvette by the end of the 15 minute monitoring period. This behavior was also reflected by the temporal instability metric shown in Figure 7 a), where unstable samples produced significantly different signals than stable ones, with the algorithm detecting instability immediately at the start of the observation period.

Once the critical pH region was identified, a high-resolution titration experiment was performed to explore the instability region (pH 5.7-5.1), as shown in Figure 7 d), e) and f). The first signs of instability appeared at pH 5.2 (cuvette 7), 60 seconds into the monitoring period. Although the sample initially appeared visually stable, sedimentation became evident at the bottom of the cuvette by the end of the monitoring period, suggesting an ongoing sedimentation process. This phenomenon is explained by the acidification of casein micelles, which typically leads to their progressive disruption and the subsequent release of calcium phosphate (HadjSadok et al., 2008). Since calcium phosphate is insoluble in this pH range, it tends to sediment if the viscosity of the continuous phase is too low to keep it suspended. While the microparticles dispersed in the liquid were initially imperceptible to the human eye, the Laplacian-based algorithm successfully detected this instability. The last unstable sample exhibited evident aggregation, with macroparticles moving freely through the liquid. This was pronounced by a sharp increase in the measured instability metric as shown on Figure 7 d). In contrast, for sedimentation observed at pH 5.2, the instability metric followed a different pattern, rising initially and then stabilizing around the 5–6 minute mark, indicating the end of the sedimentation process. Stable samples generally remained below the threshold, with occasional readings exceeding the limit. Although our algorithm takes this phenomenon into the account to avoid the detection of false positives, prolonged monitoring of such samples may offer further insights into long-term stability.

3.3. Experiment Repeatability

The repeatability of the robotic experimental process was validated through a high-resolution titration of MPC within the pH range of 5.7–5.1, as shown in Figures 8 a) and b). The identical experiment was performed three times, each using an independently prepared sample from the same protein batch. In all MPC experiments, the starting

	Instability pH	**Titrant Volume (mM of added H^+)**	**Total Duration (min.)**
Low Res. Exp.	5.13	9.4	25.1
High Res. EXP 1	5.20	9.1	30.1
High Res. EXP 2	5.19	8.1	29.1
High Res. EXP 3	5.20	8.6	31.5

Table 2: Comparison of key metrics across low and high-resolution titration experiments.

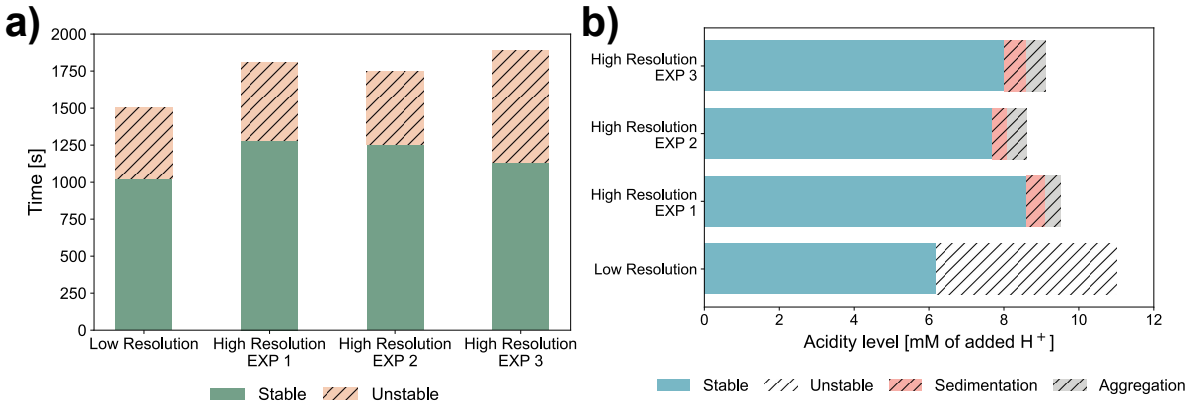

Figure 8: Repeatability of the experimental process for low (0.5 pH step) and high resolution (0.1 pH step) experiments. (a) Duration of the experiments, including the time required to reach the instability. (b) The amount of 0.1 mol Hydrochloric Acid (HCl) added to reach the instability point.

solution pH measured 7.18, the last stable pH was 5.3 and the first instability occurred consistently at pH 5.2 as shown in Table 2. The amount of titrant required to reach the instability point averaged 8.6 mM, with a variation of ±6%.

Each trial required the observation of eight cuvettes, with an average experiment duration of 30 minutes and a variation of 2.5 minutes, typically detecting instability around the 20-minute mark. In contrast, the low resolution experiment, which monitored only six cuvettes, was completed in 25 minutes. The primary factor influencing the total experiment duration was the fixed 15-minute observation period. However, when the number of cuvettes was constant, variation in experiment duration occurred due to differences in how efficiently the controller reached the pH targets during titration.

4. Discussion

The combined robotic platform and Laplacian-based computer vision algorithm reliably and autonomously detected both subtle and pronounced physical instabilities in protein dispersions. Across all experiments, the system repeatedly identified the instability pH of MPC at 5.2, consistent with established casein micelle behavior (Ju & Kilara, 1998), (S. Wu et al., 2019). Instability was detected within the first minute of monitoring in all cases, suggesting that using a finer pH step may reveal additional transitions that develop only over longer observation periods. In terms of repeatability, the titrant volume required to reach the instability point varied by ±6%, reflecting the limits of the pH-control and dosing precision. Although temporal noise in the Laplacian metric remained low (1%), the instability threshold derived from stable samples (3.5%) may shift between experiments or formulations, requiring frequent recalibration.

	Proposed System	**DLS (Cuvette)**	**DLS (Well-plate)**
Sample Format	Cuvette	Cuvette	96-384 well-plate
Sample Volume	4 mL	4 mL	20-50 µL/well
Monitoring Capability	Parallel	Sequential	Sequential
Concurrent Samples	10	1	1
Samples Per Hour	20	10-20	30-60

Table 3: Comparison of key metrics for the proposed, DLS-cuvette and DLS-well-plate systems.

When compared to similar platforms (Dauer, Kamm, et al., 2021), the developed robotic system offers an accessible alternative by using standard CMOS cameras rather than advanced instruments such as DLS (Table 3). It also provides continuous, real-time monitoring, allowing the temporal evolution of instability to be continuously observed rather than captured only at discrete time points. However, the system comes with several limitations. Each formulation requires a two-stage titration, a coarse scan followed by a fine scan, which increases experimental time. Detection is restricted to features that produce visible contrast, and the system is sensitive to optical artifacts such as reflections or cuvette condensation at elevated temperatures. Variations in illumination can also reduce consistency and comparability across experiments and camera setups. These constraints limit the system's suitability for many pharmaceutical and bioscience applications, where sub-visible particle analysis and precise quantification are required. Despite these limitations, the ability to objectively track visual changes over time makes the system well suited for early-stage formulation development in food science, where stability assessments have traditionally relied on subjective human observation.

While these initial results validate the concept, further verification is required. Further testing should include transparent systems (e.g. whey), colored samples (e.g. pea protein), and darker formulations (e.g. coffee) as well as multi-ingredient dispersions such as plant-based milks. With the automated system enabling large-scale data collection, future work can explore deep learning approaches such as Convolutional Neural Networks (CNNs) trained to identify visual patterns linked to dispersion stability. Additionally, the current computer-vision pipeline can be expanded by investigating alternative methods such as Fourier Transform analysis. In contrast to the Laplacian, which emphasizes local intensity changes, the Fourier approach captures global variations and is less sensitive to noise and illumination changes (Szeliski, 2022). A hybrid framework combining Laplacian and Fourier-based metrics could further enhance stability assessment by leveraging the complementary strengths of both local and global feature analysis.

From a hardware perspective, translating this proof-of-concept into an industrial system will require improvements in dosing accuracy, system robustness, and integration. Incorporating a multiplex syringe pump could improve dosing precision, increase the number of reagents that can be handled, and reduce hardware complexity by removing one Cartesian arm. Beyond standalone operation, this system could also be integrated into larger robotic workflows that combine automated sample preparation and testing. Alternatively, the computer vision module could operate independently as a standalone monitoring tool while relying on manual titration.

5. Conclusions

We have introduced a robotic platform for automated visual stability monitoring in liquid systems, combining autonomous sample preparation with Laplacian-based instability detection. The robotic system autonomously performs titration and pipetting tasks, monitors samples stored in cuvettes, and applies a Laplacian-based computer vision algorithm for real-time instability detection. Across several experiments performed on milk protein dispersions, the system reliably detected not only large-scale aggregation, but also subtle physical instability phenomena such as sedimentation. These instabilities were identified even when particles were invisible to the human eye, achieving earlier detection than a trained human observer. Protein aggregation was consistently detected at pH 5.1 after 30 seconds of monitoring, while sedimentation was observed at pH 5.2 at

the 60-second mark. Each experiment typically lasted about 30 minutes, with a variation of 2.5 minutes, primarily influenced by the efficiency of the pH adjustment controller.

By combining robotic automation with computer vision, we present a cost-effective, medium-to-high throughput alternative to predominantly manual experimental processes. Robotic automation ensures a highly efficient and repeatable experimentation, while the integrated computer vision algorithm, capable of detecting both micro and macroscopic physical instabilities, enables real-time monitoring and robust data capture even across different sample batches. Future research will focus on validating the system across a wider range of formulations with differing optical and physical properties, including variations in transparency, color, and aggregation behavior. The computer vision pipeline will be expanded through benchmarking of complementary algorithms beyond the Laplacian method, such as Fourier analysis, image classification, and neural networks. In the longer term, advances in hardware design and system integration could transform this proof of concept into an industrial-scale platform for high-throughput formulation screening.

ACKNOWLEDGMENT

This project was supported by the EU's Horizon 2020 research and innovation program under the Marie Skłodowska Curie grant agreement No 945363.

References

Abolhasani, M., & Kumacheva, E. (2023). The rise of self-driving labs in chemical and materials sciences. *Nature Synthesis*, *2*(6), 483–492.

Alexander, M., & Dalgleish, D. G. (2006). Dynamic light scattering techniques and their applications in food science. *Food Biophysics*, *1*, 2–13.

Alexovič, M., Dotsikas, Y., Bober, P., & Sabo, J. (2018). Achievements in robotic automation of solvent extraction and related approaches for bioanalysis of pharmaceuticals. *Journal of Chromatography B*, *1092*, 402–421.

Alexovič, M., Urban, P. L., Tabani, H., & Sabo, J. (2020). Recent advances in robotic protein sample preparation for clinical analysis and other biomedical applications. *Clinica Chimica Acta*, *507*, 104–116.

Bhargava, A., & Bansal, A. (2021). Fruits and vegetables quality evaluation using computer vision: A review. *Journal of King Saud University-Computer and Information Sciences*, *33*(3), 243–257.

Bovik, A. C. (2010). *Handbook of image and video processing*. Academic press.

Burger, B., Maffettone, P. M., Gusev, V. V., Aitchison, C. M., Bai, Y., Wang, X., Li, X., Alston, B. M., Li, B., Clowes, R., et al. (2020). A mobile robotic chemist. *Nature*, *583*(7815), 237–241.

Chaudhuri, R., Cheng, Y., Middaugh, C. R., & Volkin, D. B. (2014). High-throughput biophysical analysis of protein therapeutics to examine interrelationships between aggregate formation and conformational stability. *The AAPS journal*, *16*(1), 48–64.

Cosgrove, T. (2010). *Colloid science: Principles, methods and applications*. John Wiley & Sons.

Dauer, K., Kamm, W., Wagner, K. G., & Pfeiffer-Marek, S. (2021). High-throughput screening for colloidal stability of peptide formulations using dynamic and static light scattering. *Molecular Pharmaceutics*, *18*(5), 1939–1955.

Dauer, K., Pfeiffer-Marek, S., Kamm, W., & Wagner, K. G. (2021). Microwell plate-based dynamic light scattering as a high-throughput characterization tool in biopharmaceutical development. *Pharmaceutics*, *13*(2), 172.

Den Engelsman, J., Garidel, P., Smulders, R., Koll, H., Smith, B., Bassarab, S., Seidl, A., Hainzl, O., & Jiskoot, W. (2011). Strategies for the assessment of protein aggregates in pharmaceutical biotech product development. *Pharmaceutical researc Wangh*, *28*, 920–933.

Dickinson, E. (2015). Colloids in food: Ingredients, structure, and stability. *Annual review of food science and technology*, *6*(1), 211–233.

Everett, D. H. (2007). *Basic principles of colloid science*. Royal society of chemistry.

Gonzalez Viejo, C., Fuentes, S., Torrico, D., Howell, K., & Dunshea, F. R. (2018). Assessment of beer quality based on foamability and chemical composition using computer vision algorithms, near infrared spectroscopy and machine learning algorithms. *Journal of the Science of Food and Agriculture*, *98*(2), 618–627.

Grandjean, E. (1979). Fatigue in industry. *Occupational and Environmental Medicine*, *36*(3), 175–186.

HadjSadok, A., Pitkowski, A., Nicolai, T., Benyahia, L., & Moulai-Mostefa, N. (2008). Characterisation of sodium caseinate as a function of ionic strength, ph and temperature using static and dynamic light scattering. *Food Hydrocolloids*, *22*(8), 1460–1466.

Hassoun, A., Jagtap, S., Garcia-Garcia, G., Trollman, H., Pateiro, M., Lorenzo, J. M., Trif, M., Rusu, A. V., Aadil, R. M., Šimat, V., et al. (2023). Food quality 4.0: From traditional approaches to digitalized automated analysis. *Journal of Food Engineering*, *337*, 111216.

He, Y., Xu, C., Khanna, N., Boushey, C. J., & Delp, E. J. (2013). Food image analysis: Segmentation, identification and weight estimation. *2013 IEEE international conference on multimedia and expo (ICME)*, 1–6.

Holland, I., & Davies, J. A. (2020). Automation in the life science research laboratory. *Frontiers in bioengineering and biotechnology*, *8*, 571777.

Housmans, J. A., Wu, G., Schymkowitz, J., & Rousseau, F. (2023). A guide to studying protein aggregation. *The FEBS journal*, *290*(3), 554–583.

Ju, Z. Y., & Kilara, A. (1998). Gelation of ph-aggregated whey protein isolate solution induced by heat, protease, calcium salt, and acidulant. *Journal of Agricultural and Food Chemistry*, *46*(5), 1830–1835.

Matusiak, J., & Grzadka, E. (2017). Stability of colloidal systems-a review of the stability measurements methods. *Annales Universitatis Mariae Curie-Sklodowska, sectio AA–Chemia*, *72*(1), 33.

Mcclements, D. J. (2007). Critical review of techniques and methodologies for characterization of emulsion stability. *Critical reviews in food science and nutrition*, *47*(7), 611–649.

McNally, E. J., McNally, E., & Hastedt, J. E. (2007). Protein formulation and delivery.

Milovanovic, B., Tomovic, V., Djekic, I., Miocinovic, J., Solowiej, B. G., Lorenzo, J. M., Barba, F. J., & Tomasevic, I. (2021). Colour assessment of milk and milk products using computer vision system and colorimeter. *International Dairy Journal*, *120*, 105084.

Molet-Rodríguez, A., Salvia-Trujillo, L., & Martín-Belloso, O. (2018). Beverage emulsions: Key aspects of their formulation and physicochemical stability. *Beverages*, *4*(3), 70.

Müller, S., Ilić, S., Scamarcio, V., & Hughes, J. (2023). A cartesian platform for cooperative multi-robot manipulation tasks. *2023 IEEE/RSJ International Conference on Intelligent Robots and Systems (IROS)*, 10082–10087.

Ryan, K. N., & Foegeding, E. A. (2015). Formation of soluble whey protein aggregates and their stability in beverages. *Food Hydrocolloids*, *43*, 265–274.

Schmitt, C., Bovetto, L., Buczkowski, J., Reis, G. D. O., Pibarot, P., Amagliani, L., & Dombrowski, J. (2021). Plant proteins and their colloidal state. *Current Opinion in Colloid & Interface Science*, *56*, 101510.

Shi, Y., Wang, X., Borhan, M. S., Young, J., Newman, D., Berg, E., & Sun, X. (2021). A review on meat quality evaluation methods based on non-destructive computer vision and artificial intelligence technologies. *Food science of animal resources*, *41*(4), 563.

Shrivakshan, G., & Chandrasekar, C. (2012). A comparison of various edge detection techniques used in image processing. *International Journal of Computer Science Issues (IJCSI)*, *9*(5), 269.

Sun, D.-W. (2016). *Computer vision technology for food quality evaluation*. Academic Press.

Szeliski, R. (2022). *Computer vision: Algorithms and applications*. Springer Nature.

Tadros, T. (2007). General principles of colloid stability and the role of surface forces.

Wang, Z., Hirai, S., & Kawamura, S. (2022). Challenges and opportunities in robotic food handling: A review. *Frontiers in Robotics and AI*, *8*, 789107.

Wijaya, W., Patel, A. R., Setiowati, A. D., & Van der Meeren, P. (2017). Functional colloids from proteins and polysaccharides for food applications. *Trends in Food Science & Technology*, *68*, 56–69.

Wu, D., & Sun, D.-W. (2013). Colour measurements by computer vision for food quality control–a review. *Trends in Food Science & Technology*, *29*(1), 5–20.

Wu, S., Fitzpatrick, J., Cronin, K., & Miao, S. (2019). The effect of ph on the wetting and dissolution of milk protein isolate powder. *Journal of Food Engineering*, *240*, 114–119.

Yan, X., Ma, C., Cui, F., McClements, D. J., Liu, X., & Liu, F. (2020). Protein-stabilized pickering emulsions: Formation, stability, properties, and applications in foods. *Trends in Food Science & Technology*, *103*, 293–303.

Zhu, Z., Bassey, A. P., Cao, Y., Ma, Y., Huang, M., & Yang, H. (2022). Food protein aggregation and its application. *Food research international*, *160*, 111725.